A plant proton-pumping inorganic pyrophosphatase functionally complements the vacuolar ATPase transport activity and confers bafilomycin resistance in yeast

Jose R. Perez-Castiñeira, Agustín Hernández, Rocio Drake, Aurelio Serrano

Title: A plant proton-pumping inorganic pyrophosphatase functionally complements the vacuolar ATPase transport activity and confers bafilomycin resistance in yeast

Short title: Functional complementation of yeast vacuolar H^+-ATPase by a H^+-PPase

Authors: José R. PÉREZ-CASTIÑEIRA, Agustín HERNÁNDEZ, Rocío DRAKE and Aurelio SERRANO[1]

Instituto de Bioquímica Vegetal y Fotosíntesis, Universidad de Sevilla-CSIC, Avda. Americo Vespucio, 49, 41092 Sevilla, Spain

[1] To whom correspondence should be addressed (Phone: +-34-954489525. Fax: +-34-954460065; Email: aurelio@ibvf.csic.es)

Abbreviations used: ACMA, 9-amino-6-chloro-2-methoxy acridine; FITC: fluorescein isothiocyanate; MALDI-TOF: Matrix assisted laser desorption ionisation-time of flight; MES, 2-(N-Morpholino)ethanesulphonic acid; PPi: inorganic pyrophosphate; PPase: inorganic pyrophosphatase; H^+-PPase: membrane-bound H^+-translocating inorganic pyrophosphatase; TRIS, Tris(hydroxymethyl)aminomethane

Abstract

Vacuolar H^+-ATPases (V-ATPases) are a specific class of multisubunit pumps that play an essential role in the generation of proton gradients across eukaryotic endomembranes. Another simpler proton pump that co-localises with the V-ATPase occurs in plants and many protists: the single-subunit H^+-translocating inorganic pyrophosphatase (H^+-PPase). Little is known about the relative contribution of these two proteins to the acidification of intracellular compartments. Here, we show that the expression of a chimaeric derivative of the *Arabidopsis thaliana* H^+-PPase AVP1 that is preferentially targeted to internal membranes of yeast alleviates the phenotypes associated with V-ATPase deficiency. Phenotypic complementation was achieved both with a yeast strain with its V-ATPase specifically inhibited by bafilomycin A1 and with a *vma*1 null mutant lacking a catalytic V-ATPase subunit. Cell staining with vital fluorescent dyes showed that AVP1 recovered vacuole acidification and normalised the endocytic pathway of the *vma* mutant. Biochemical and immunochemical studies further demonstrated that a significant fraction of heterologous H^+-PPase is located at the vacuolar membrane. These results raise the question of the occurrence of distinct proton pumps in certain single-membrane organelles, such as plant vacuoles, by proving yeast V-ATPase activity dispensability and the capability of H^+-PPase to generate by itself physiologically suitable internal pH gradients. Besides, they envisage new ways of engineering macrolide drugs tolerance and outline an experimental system for testing alternative roles for fungal and animal V-ATPases, other than the mere acidification of subcellular organelles.

Key words: chimaeric membrane proteins, green fluorescent protein, heterologous expression, proton-translocating inorganic pyrophosphatase, *Saccharomyces cerevisiae*, vacuolar-type adenosine triphosphatases.

INTRODUCTION

The occurrence of an electrochemical proton gradient across the internal membranes of eukaryotic cells is one of the requirements known for the correct function of the endo- and exocytic pathways [1]. Moreover, pH gradients are necessary not only for the correct functioning of the vesicle transport machinery but also for many other organellar functions, such as dissociation of ligand-receptor complexes in receptor-mediated endocytosis or glycosylation of proteins in the Golgi apparatus, among others [2]. A specific class of proton-pumping ATPases, usually called vacuolar ATPases or V-type ATPases (V-ATPases), play an essential role in the generation of these positive-inside proton gradients [1, 3]. V-ATPases were originally described in the vacuolar membrane of plants and fungi (hence their name), thereafter, they were found in many single-membrane organelles of eukaryotic cells. In addition, they have also been reported to occur at the plasma membrane of certain mammalian cell types [2]. All in all, these multi-subunit proteins fulfil important roles in diverse scenarios, both physiological and in disease, including cancer [3, 4] . Not surprisingly then, there is an active search for specific inhibitors of these pumps that could be used both in basic research and in therapeutic applications. Bafilomycin A1 was the first reported specific inhibitor of V-ATPases [5], it consists of a large macrocyclic lactone ring which places it in the macrolide antibiotic group. Unlike other eukaryotes, *Saccharomyces cerevisiae* cells can grow either in the presence of V-ATPase inhibitors [6] or when a null mutation occurs in one of the genes encoding certain subunits of the V-ATPase complex [1]. However, they show a range of conditional-lethal phenotypes and thus become very sensitive to neutral/alkaline pHs [6, 7], high extracellular calcium concentrations [8] and certain metal cations such as zinc [9]; actually, the combination of sensitivity to high pH and extracellular calcium is widely accepted as the most characteristic Vma^- phenotype [1].

V-type ATPases are very complex multi-subunit pumps that contain both membrane-bound and peripheral components. This paradoxical complexity, in comparison to other transporters, has been recently justified by proposing moonlighting functions of some subunits or even whole domains of the V-ATPases [10, 11]**.** However, to study non-transport functions of V-ATPases is a complicated task if organelle acidification is not taken over by some other protein(s). Strikingly, this situation may be the natural scenario in plant cells and many protists where V-ATPases coexist with alternative proton pumps. However, to date, no work has proven that V-ATPases can be unambiguously substituted by any other proton pump *in vivo*.

Proton-translocating inorganic pyrophosphatases (H^+-PPases) are a type of homooligomeric membrane-embedded proteins containing a single highly hydrophobic subunit type that couples the energy obtained in the hydrolysis of inorganic pyrophosphate (PPi) to the transport of protons across biological membranes [12-14]. They conform the structurally simplest class of primary proton pumps known to date, and the last one established, in the middle of the 80´s. H^+-PPases are reportedly located in cell membrane vesicles and acidocalcisomes of prokaryotes and diverse acidic single-membrane organelles (acidocalcisomes, lysosomes, vacuoles) of certain eukaryotes: protists and plants [13, 15-17]. H^+-PPases seem to co-localise with V-ATPases in those eukaryotes where they occur [18], thus, one point of discussion is the physiological significance of this apparent functional redundancy and if H^+-PPases contribute in varying degrees to the generation of proton gradients under diverse physiological scenarios.

We recently reported that translational fusions with certain N-terminal signal peptides enhance the expression levels and/or alter the subcellular distribution of diverse H^+-PPases

heterologously expressed in *S. cerevisiae*. When this approach was applied to the vacuolar H^+-PPase AVP1 from *Arabidopsis thaliana*, a protein expressed at moderate levels in yeast in its natural form [19], its subcellular distribution was altered; thus, chimaeric proteins constructed by fusing the N-terminal signal sequence of the H^+-PPase from the protist *Trypanosoma cruzi* [20] to AVP1 were shown to preferentially accumulate in intracellular acidic vesicles [21] . In this paper, we show that the expression of such internal membranes-targeted chimaeric AVP1 derivative confers yeast resistance to the antibiotic macrolide bafilomycin A1, a specific V-ATPase inhibitor. Further experiments performed with a yeast *vma* mutant defective in its V-ATPase activity demonstrated that the H^+-PPase acts by functionally complementing the transport function of the former proton pump. These results raise again the question of the presence of both proton pumps in certain organelles, such as the plant vacuole. Potential applications of this system in order to elucidate the roles of V-ATPases and/or H^+-PPases are also discussed.

EXPERIMENTAL

Yeast strains

YPC3 mutant strain was generated from *S. cerevisiae* haploid strain W303-1A (MATa, *ade2-1 can1-100 his3-11,15 leu2-3,112 trp1-1*, *ura3-1*) by the single-step transplacement procedure as described elsewhere [21]. This mutant has the *IPP1* gene coding for the cytosolic soluble inorganic pyrophosphatase under the control of the yeast galactokinase (*GAL1*) promoter. YPC4 was generated from *S. cerevisiae* mutant RS-1144 (W303-1A *vma1::LEU2*) by following the same procedure. Mutant RS-1144, generously provided by Prof. Ramón Serrano (Universidad Politécnica de Valencia, Spain), had been derived from strain W303-1A by disrupting its *VMA1 (TFP1*) gene with the yeast *LEU2* cassette [22]. The *VMA1* gene of *Saccharomyces cerevisiae* is translated by protein splicing into two different proteins: the 69-kD catalytic subunit of the vacuolar H^+-ATPase and a 50-kD DNA endonuclease [23]. Vacuolar protease-deficient mutant BJ5457 was generously donated by Prof. Andrés Aguilera (Universidad de Sevilla, Spain), this mutant carries mutations both in the *PEP4* gene and the *PRB1* gene, coding for the yeast vacuolar proteases Proteinase A (PrA) and Proteinase B (PrB), respectively [24].

Transformation of YPC3 and YPC4

S. cerevisiae mutant strains YPC3 and YPC4 were transformed with plasmids pAVP1, pTcAVP1, and pTcGFPAVP1 by using the method of Schiestl and Gietz [25]. All plasmids are 2 µm-based derivatives of the *URA*3-containing *E. coli/S. cerevisiae* shuttle plasmid pRS699 [26], as previously described [21; Supplementary Table S2 at www.BiochemJ.org/bj/426/bj4260147add.htm]. These plasmids bear the yeast *PMA1* promoter for constitutive expression of inserts [26]. Three different constructs were made using the sequence coding for the K^+-dependent H^+-PPase from the higher plant *A. thaliana* (*AVP1*): pAVP1, carrying an intron-less open reading frame construct of AVP1; pTcAVP1, a 5' in-frame fusion of the sequence coding for the N-terminal signal peptide of the *Trypanosoma cruzi* H^+-PPase (TcVP) with that of AVP1, and pTcGFPAVP1, an in-frame fusion where the sequence coding for the yeast-enhanced green fluorescent protein (yEGFP) is placed between the coding sequence of TcVP N-terminal signal peptide and that of *AVP1*. In addition to these, plasmids pIPP1, bearing the whole open reading frame encoding the cytosolic soluble inorganic pyrophosphatase from yeast (*IPP1*), and pVMA1, bearing the genomic sequence of *VMA1* coding for the A catalytic subunit of the yeast V-ATPase, were constructed using the above mentioned expression plasmid backbone **(See scheme S1)**. YPC3 and YPC4 cells were

initially grown at 30 °C in galactose-containing synthetic medium [27] devoid of histidine (YPC3) or histidine and leucine (YPC4); transformants were selected by growing cells on 2% agar plates in culture medium without histidine and uracil (YPC3) or without histidine, leucine and uracil (YPC4). 0.5 M sorbitol was added to the plates were transformants of YPC4 were selected as an osmotic protectant.

Phenotype complementation tests

Complementation studies were performed by pre-inoculating 2 ml of galactose-containing selective medium with transformed cells from the plates and growing overnight at 30 ºC with agitation (200 r.p.m.). The following day, 2 ml of glucose-containing selective medium or YPD were inoculated with 20 µl (1:100 dilution) of cells previously grown on galactose and allowed them to grow as described. This treatment is necessary to bring down the pyrophosphatase activity associated to Ipp1p [28]. After overnight growth on glucose, ten-fold serial dilutions of the cultures were made in sterile water and 5 µl drops of each dilution were spotted onto YPD and YPGal agar plates containing 50 mM TRIS-MES adjusted to pH 5.5, 7.5 or 8. 100 mM $CaCl_2$ or 4 mM $ZnCl_2$ was added to the plates at pH 5.5 where indicated. Plates were typically grown at 30 ºC for two to five days.

Fluorescence microscopy

Vacuolar lumen acidification was assessed by fluorescence staining with quinacrine as reported elsewhere [29]. Cells were visualized after 10 minutes of fluorophore accumulation with a fully automated Leica DM6000B microscope (Leica Microsystems, Wetzlar, Germany) with fluorescein isothiocyanate (FITC) green fluorescence filters (excitation filter 480/40 nm, dichromatic mirror 505 nm, suppression filter 527/30 nm), a 100x objective and equipped with a cooled CCD camera (ORCA-AG, Hamamatsu Photonics, Hamamatsu, Japan). Vacuolar membrane labelling was carried out with the vital lipophilic dye FM4-64 as previously described [29]. Cells were visualized 30 minutes after incubation with the dye as described above, except that Texas Red filters (excitation filter 560/40 nm, dichromatic mirror 595 nm, suppression filter 645/75 nm) were utilized. In all cases, cells were also viewed under differential interference contrast (DIC) microscopy to observe cell morphology.

Isolation of yeast vacuolar membranes

Colonies of transformed YPC4 cells were collected from a plate and liquid-grown up to stationary phase in galactose-containing selective medium; then, 4 ml of stationary cultures were used to inoculate 400 ml of YPD adjusted to pH 5.5 with 50 mM TRIS-MES and grown overnight to early log phase (Abs 660 nm approx. 1). Yeast vacuoles were obtained from these cultures by the method of Roberts et al. [30]

Isolation of total membrane fractions from yeast

Preparation of membrane fractions from YPC4 cells transformed with the different plasmids were obtained by a modification of a method previously described [21]: yeast colonies were collected from a plate and liquid-grown up to stationary phase in galactose-containing selective medium; then, 4 ml of stationary cultures were used to inoculate 400 ml of YPD. After overnight growth, cells were sedimented by centrifugation at 700 ***g*** for 10 min, washed thoroughly with water, resuspended in 5 ml of ice-cold buffer A (25 mM Tris-HCl, pH 8, 10% glycerol, 4 mM β-mercaptoethanol, 2 mM DTT, 2 mM EDTA, 10 mM $MgCl_2$, 1 mM benzamidine, 2 mM ε-aminocaproic acid, 1 mM PMSF), and homogenized by vigorous shaking with glass beads. The homogenate was diluted up to 25 ml with buffer B (10 mM

Tris-HCl, pH 7.6, 10% glycerol, 2 mM DTT, 1 mM EDTA) and centrifuged for 10 min at 700 ***g*** to remove beads and debris. The resulting supernatant was centrifuged for 30 minutes at 120,000 ***g*** thus yielding a total membrane pellet. This pellet was homogenized in stripping buffer (60 mM Tris-HCl, pH 8, 12% glycerol, 0.72 M KCl, 1.2 mM $CaCl_2$) [31] and centrifuged for 20 minutes at 120,000 ***g***. This pellet was subsequently washed with buffer B and centrifuged (20 min, 120,000 ***g***). The final pellets were resuspended and homogenized in 1 ml of buffer B.

Pyrophosphatase activity and H^+-translocation assays

Membrane-associated PPase activity was measured by spectrophotometric detection of released phosphate [32]. Proton-translocation activities were assayed by monitoring the fluorescence quenching of 9-amino-6-chloro-2-methoxy acridine (ACMA) [33]. Statistical significance of the differences observed between sets of activity data was determined by Student's unpaired *t* tests using the application available at http://graphpad.com/quickcalcs/ttest1.cfm.

Western blotting and total protein estimation

Western blots were carried out after SDS-PAGE as described elsewhere [34]. For immunodetection of H^+-PPases, an affinity-purified polyclonal antibody raised in rabbit against the membrane-bound PPase (TVP) from the bacterium *Thermotoga maritima* [35] was utilised at 1:200 dilution. For Vma1p, GFP and Pma1p immunodetections commercial monoclonal antibody 8B1 (Molecular Probes, Eugene, OR, USA), a polyclonal "Living Colors" antibody from BD Biosciences (Franklin Lakes, NJ, USA) and a polyclonal antibody generously provided by Prof. Ramón Serrano (Universidad Politécnica de Valencia, Spain) were used, respectively, all of them at 1:2000 dilution. Total protein concentration was estimated by the Bradford method [36] with ovalbumin as a standard.

RESULTS

Chimaeras of AVP1 bearing the N-terminal domain of TcVP induce bafilomycin resistance in YPC3 cells

YPC3 is a yeast mutant whose *IPP1* gene coding for the essential cytosolic inorganic pyrophosphatase is under the control of the galactokinase (*GAL1*) promoter; therefore, these cells are non-viable when glucose is present as a carbon source. It has been previously shown that plant and bacterial membrane-bound H^+-translocating PPases can functionally complement the yeast cytosolic sPPase (Ipp1p), especially, when fused to certain N-terminal signal peptides [21, 28]. Addition of macrolide bafilomycin A1 to YPC3 cells transformed with different plasmids bearing constitutively-expressed genes coding for soluble or membrane-bound PPases resulted in sensitivity to neutral/alkaline pH and to the divalent cations Ca^{2+} and Zn^{2+}, when grown on galactose (Fig. 1), that is, when Ipp1p is expressed. On the contrary, when cells were grown on glucose in the presence of bafilomycin, those expressing different chimaeric derivatives of AVP1, the K^+-dependent H^+-PPase from the higher plant *A. thaliana*, recover the capacity to grow at pH 7.5-8.0 (Fig. 1A). In the presence of 100 mM calcium at pH 5.6, some growth was observed in YPC3 cells overexpressing Ipp1p although they became significantly sensitive to this cation. Cells expressing the different AVP1 chimaeras showed a somewhat smaller sensitivity to this $CaCl_2$ (Fig. 1B). In the presence of zinc ions only those cells transformed with plasmids pTcAVP1 and pTcGFPAVP1 expressing internal membranes-targeted chimaeras could grow after four days,

especially the latter (Fig. 1B).

Chimaeras of AVP1 bearing the N-terminal domain of TcVP reverts the sensitivity to neutral/alkaline pH, calcium and zinc of YPC4 Vma1$^-$ cells

In order to fully ascertain that the observed bafilomycin A1 tolerance was actually brought about by complementation of V-ATPase proton transport activity, similar experiments to those described above were performed with YPC4 cells. This mutant also has *IPP1* under the control of the *GAL1* promoter but, additionally, it has the gene coding for the catalytic subunit VMA1 of the vacuolar H^+-ATPase disrupted. YPC4, like YPC3, is unable to grow on glucose, but, as expected, when grown on galactose it exhibits the typical range of Vma$^-$ phenotypes: very high sensitivity to neutral/alkaline pHs and to Ca^{2+} and Zn^{2+} cations (Figs. 2A and 2B). However, when YPC4 cells were transformed with AVP1 and its chimaeric derivatives, they recovered the capacity to grow on glucose at pH 5.5 and 7.5, especially in the case of the TcGFPAVP1 chimaera. In the presence of Ca^{2+}, only cells transformed with plasmids pTcAVP1 and pTcGFPAVP1 were able to grow, whereas only the latter showed growth in the presence of Zn^{2+}. Again, as in the case of YPC3 with bafilomycin A1, the construction bearing the gene coding for Ipp1p could only support growth on glucose at pH 5.6 and in the absence of divalent cations. On the other hand, transformation of YPC4 with *VMA1* resulted in the reversal of the phenotypes associated with the disruption of this gene only in the presence of galactose (Fig. 2, A and B).

Expression of TcGFPAVP1 allows acidification of vacuoles in YPC4 cells

To verify that AVP1 and its derivatives were able to promote acidification of internal compartments, we analysed the accumulation of quinacrine, a vital dye that concentrates in acidic lumina. Fig. 3 shows typical patterns of quinacrine accumulation in vacuoles of YPC4 cells transformed with the different constructions tested. No internal acidification could be observed in cells expressing the soluble cytosolic PPase Ipp1p whereas cells expressing AVP1 and TcAVP1 showed a punctated pattern of green fluorescence suggesting acidification of prevacuolar/endosomal compartments. In contrast to this, cells transformed with the plasmid pTcGFPAVP1 showed a different fluorescence pattern, with a clear vacuolar accumulation of quinacrine just like YPC4 cells transformed with plasmid pVMA1 grown in galactose. The former cells showed a punctated green fluorescence pattern, corresponding to the TcGFPAVP1 polypeptide, when visualised in the absence of quinacrine (see below). It is important to point out that some of the cells transformed with pTcGFPAVP1 exhibited clusters of smaller vacuoles rather than the single large vacuole usually observed in cells expressing Vma1p (see Fig. 3). These results are in agreement with the previously presented drop tests (cf. Figs. 1 and 2), which show comparatively higher growth of TcGFPAVP1 expressing clones at neutral/alkaline pHs and in the presence of Ca^{2+}/Zn^{2+}, these tolerance phenotypes being strictly dependent of physiologically competent acidic vacuoles.

Expression of all AVP1 derivatives allows normal internalization of the vital dye FM4-64

The vital fluorescent dye FM4-64 binds to the plasma membrane and follows the endocytic pathway to reach the vacuole [29]. FM4-64 internalization has been shown to be severely impaired in *vma* mutants [37]. Figure 4 shows labelling of vacuole membranes in YPC4 cells after incubation with FM4-64 during 30 minutes. It can be observed that cells expressing the AVP1 and TcGFPAVP1 proteins have their vacuoles clearly labelled, whereas cells expressing TcAVP1 showed labelling of vacuoles and other smaller vesicles. Control cells expressing Vma1p also showed a clear pattern of vacuolar membrane staining. No internal labelling was

obtained in cells transformed with pIPP1. Cells transformed with pTcGFPAVP1 were also visualised with a green (FITC) fluorescence filter showing a punctated pattern that suggested either a preferential localization of TcGFPAVP1 in internal membranes other than the vacuolar membrane or a degradation of the GFP moiety by vacuolar proteases (Fig. 4B), a possibility that was subsequently studied by using a vacuolar protease-deficient mutant (see below). In some of these cells, clusters of small acidic vesicles were also observed. This effect had previously been described with YPC3 cells [21] .

Membrane-bound H^+-PPases are present in YPC4 vacuoles

In order to check whether the different natural and chimaeric plant H^+-PPases expressed in YPC4 cells were localised in the vacuoles, activity assays and immunodetection experiments were carried out with purified vacuole preparations obtained from YPC4 cells transformed with the different plasmids above described. Cells transformed with pTcGFPAVP1 showed a characteristic trace of ACMA fluorescence quenching that was dependent on the addition of PPi, this quenching was reversed by the addition of the H^+/K^+ ionophore nigericin. Smaller quenching rates were obtained with cells transformed with pTcAVP1 and pAVP1 (Fig. 5A). Vacuoles from cells transformed with pVMA1 did not show PPi-dependent ACMA quenching, just like cells transformed with plasmids pRS699b and pIPP1 (not shown). When ATP-dependent proton transport was recorded, only vacuoles isolated from cells transformed with plasmid pVMA1 exhibited ACMA quenching (Fig. 5A). This quenching was sensitive to bafilomycin A1 (not shown). Membrane-associated PPase activity levels determined for vacuolar membranes obtained from the different YPC4 transformants were consistent with the H^+-translocation data (Fig. 5B), thus, no PPase activity was detected in samples obtained from cells transformed with plasmids pRS699b, pIPP1 and pVMA1. Samples from cells expressing the different AVP1 chimaeras did show PPase activity that was increased by the addition of K^+, a feature of AVP1 [19]. Immunodetection in Western blots of vacuolar membranes of the diverse native and chimaeric plant H^+-PPases studied in this work (Fig. 5C) gave somewhat unpredicted results despite the use of protease inhibitors cocktails during the isolation procedure, thus, a polypeptide of the expected size for the native AVP1 protein (ca. 72 kDa) was obtained in the case of cells transformed with pAVP1, pTcAVP1 and pTcGFPAVP1; additionally, another band of ca. 64 kDa was present in these preparations. The relative amounts of H^+-PPases immunodetetcted in these preparations were, however, in accordance with the estimated activity values. A minor band of ca. 120 kDa, the size expected for TcGFPAVP1, could also be detected only in samples obtained from cells transformed with plasmid pTcGFPAVP1 (cf. Fig. 5C).

Vacuolar proteases are involved in the processing of native AVP1 and its chimaeric derivatives targeted to the vacuolar membrane

The possibility that AVP1 and its chimaeras might be subjected to proteolytic processing by vacuolar proteases *in vivo* was investigated by utilising the vacuolar protease deficient yeast mutant BJ5457 [24]. Immunodetection analyses carried out with total membrane preparations obtained with mutants YPC4 and BJ5457 transformed with plasmids pAVP1, pTcAVP1 and pTcGFPAVP1 using an antibody against a bacterial membrane-bound PPase (anti-TVP) showed remarkable results (Fig. 6A). Thus, in the case of YPC4, a polypeptide of ca. 72 kDa was detected in all cases, although in cells transformed with pTcGFPAVP1, two more bands of ca. 120 kDa and 64 kDa were clearly recognised by anti-TVP. Peptide mass fingerprint analysis of the 120 kDa polypeptide by MALDI-TOF mass spectrometry showed that it actually corresponded to a fusion between GFP and AVP1 (not shown). Consistently, an

antibody against GFP (anti-GFP) only recognised the 120 kDa band. In the case of mutant BJ5457, anti-TVP antibody recognised polypeptides of ca. 72 kDa only in preparations obtained with cells transformed with plasmids pAVP1 and pTcAVP1, whereas a single polypeptide of ca. 120 kDa was detected in membranes of cells transformed with plasmid pTcGFPAVP1. Anti-GFP could only detect the latter (Fig. 6A).

Analysis of membrane-associated PPi hydrolytic activity showed that, in YPC4, the presence of GFP at the N-terminus of AVP1 increased the specific activity of the resulting protein 3 to 4-fold with respect to AVP1 and TcAVP1. In mutant BJ5457 the specific PPase activities associated to AVP1, TcAVP1 and TcGFPAVP1 were significantly increased with respect to the same proteins expressed in YPC4. The increases were much higher in the cases of AVP1 (approx. 6-fold) and TcAVP1 (approx. 4-fold) than in the case of TcGFPAVP1 (approx. 1.7-fold) (Fig. 6B).

Fluorescent microscopy visualisation of YPC4 and BJ5457 cells transformed with plasmid pTcGFPAVP1 remarkably showed different patterns of green fluorescence distribution, thus, in YPC4 cells a punctated pattern was observed, suggesting a preferential accumulation of green fluorescence in internal membrane systems other than the vacuolar membrane. On the contrary, green fluorescence mostly associated to the latter was clearly observed in BJ5457 cells (Fig. 6C).

DISCUSSION

In previous works, we emulated in yeast the cytosolic PPi metabolism of the plant cell, i. e., absence of a soluble cytosolic PPase, so that the PPi generated by the anabolism was efficiently hydrolysed by a membrane-embedded PPi-dependent proton pump [21, 28] . In this paper, we have taken one step forward using a metabolic background in which the ATP-dependent proton pump of yeast internal membranes, the V-ATPase, has been either chemically inhibited or functionally impaired by mutation of a gene encoding an essential catalytic subunit. The results obtained strongly suggest that a distinct type of PPi-dependent proton pump can efficiently substitute for the V-ATPase of *S. cerevisiae* in diverse physiological scenarios. Thus, overexpression of the K^+-dependent H^+-PPase from the higher plant *A. thaliana*, a protein that occurs along with a V-ATPase in plant tonoplast [18], alleviates the range of phenotypes associated with the lack of the latter. The presence of an appropriate N-terminal domain proved to be important in order to observe the optimal phenotypic complementation in our system. The N-terminal domain with signal sequence features of a protistan H^+-PPase, when fused to AVP1, alters the subcellular distribution of the latter so that it becomes preferentially located in internal membranes of yeast [21]. Not surprisingly, as shown in this work, chimaeric proteins of AVP1 constructed with that signal peptide (TcAVP1 and TcGFPAVP1) functionally substituted for the V-ATPase more efficiently than the native AVP1 protein with no extra N-terminal domain. The difference in favour of TcGFPAVP1 versus TcAVP1 is probably due to the higher overall expression levels attained by the former (see below), actually, under non-restrictive conditions towards Vma^- defects TcGFPAVP1 supports growth of YPC4 more efficiently than TcAVP1 (Fig. 2A) which means that the former is more efficient at complementing the phenotype associated with the absence of Ipp1p. Addition of GFP at the N-terminus of some membrane proteins has been previously reported either because it stabilises proteins expressed in heterologous systems or because the presence of GFP at the C-terminus yields polypeptides with no activity [21, 38, 39]. In fact, both assumptions are true for the plant H^+-PPase AVP1 expressed in yeast, as this and our previous work demonstrate [21].

The results with both bafilomycin-treated YPC3 and YPC4 cells also showed that no version of heterologously-expressed AVP1 was able to complement Vma^- phenotypes in galactose, even though the corresponding genes are under the control of the constitutive *PMA1* promoter. Similarly, when the parental strains (bafilomycin-treated W303-1A and RS-1114) were transformed with the same plasmids no complementation of the V-ATPase by AVP1 was observed either on galactose or on glucose (not shown). These results suggested that AVP1 cannot pump protons when the soluble PPase is present in the cytosol probably due to the competition for the substrate, therefore, it was necessary to bring down the activity of the latter to negligible levels in order to have the former efficiently working *in vivo*. YPC3 and YPC4 were designed and generated so that this could be accomplished by transferring the cells from galactose to glucose and allowing them to grow for several hours. Actually, this reflects the metabolic scenario in cells of plant green tissues, where sPPases are restricted to energy-linked organelles (mitochondria, chloroplasts) and, probably, nuclei [17], although it must be mentioned that other PPi-utilising enzymes involved in central carbon metabolism, such as a PPi-dependent phosphofructokinase, are also present in the plant cell cytosol [40]. All in all, these data suggest that the presence of active soluble PPases is incompatible with H^+-PPase functions and helps to understand why the former are not found in the cytosol of eukaryotic cells if H^+-PPases are present in endomembranes.

Acidification of internal compartments of YPC4 cells was studied with the fluorescent probe quinacrine, which accumulates in acidic vacuoles. TcGFPAVP1 was able to acidify the vacuole in YPC4 cells although it also seemed to induce some fragmentation of this compartment. This has already been reported for YPC3 cells and may be related to the accumulation of this heterologous chimaeric protein in the internal compartments of yeast cells [21]. It should be noted in this respect that a more or less severe vacuolar fragmentation takes place in yeast under several, and not necessarily pathological, scenarios. On the contrary, cells transformed with AVP1 and TcAVP1 showed a punctated pattern of quinacrine accumulation which probably means acidification of prevacuolar/endosomal vesicles. This pattern was more significant in the case of TcAVP1, probably due to the effect of the addition of the N-terminal signal domain added to the latter that favours accumulation of this chimaeric protein in internal membranes of yeast [21]. In the presence of quinacrine cells expressing TcGFPAVP1 only exhibited the green fluorescence associated with the dye; however, these cells were also expected to show green fluorescence due to the GFP. Consequently, they were also visualised in the absence of quinacrine showing in this case a punctated pattern of fluorescence (see below). This suggests that quinacrine fluorescence masks that of GFP in our system when both are monitored simultaneously.

Results with FM4-64 are consistent with those obtained with quinacrine in the case of TcGFPAVP1; however, they further suggest that full acidification of the vacuole may not be absolutely essential to have the endocytic system operational at the right pace, acidification of the prevacuolar/endosomal compartments being sufficient. The fact that the green fluorescence observed in YPC4 cells transformed with plasmid pTcGFPAVP1 does not necessarily colocalise with the red fluorescence associated with acidic vesicles further suggests that either TcGFPAVP1 polypeptide is not significantly translocated to the vacuolar membrane or the GFP moiety of this chimaera has been lost, presumably by proteolysis.

Biochemical analysis of vacuolar membrane preparations from YPC4 transformed with the different plasmids tested showed that AVP1 and all its chimaeric derivatives were heterologously expressed and located, at least partially, in the vacuoles, as demonstrated by the data of membrane-associated H^+-translocating and PPase activities as well as by immunodetection analysis of vacuolar membrane preparations. Activity data were consistent

with the phenotypes observed, thus, TcGFPAVP1 showed higher PPase and H^+-translocating activities than TcAVP1 which, in turn, produced higher activies than the native AVP1. Immunodetection with antibody anti-TVP revealed that TcAVP1 and TcGFPAVP1 gave higher expression levels in this compartment than AVP1. This is consistent with previous reports about the role of the N-terminal signal domain of *T. cruzi* H^+-PPase on the subcellular distribution of AVP1 [21]. On the other hand, a significant processing of all the proteins examined was also found, actually, only a tiny amount of a polypeptide of ca. 120 kDa, corresponding to a fusion of GFP and AVP1, was detected and another band of ca. 64 kDa was consistently observed in all cases. This evidence suggested that vacuolar proteases may be involved in the cleavage of AVP1 and its derivatives, with a concomitant degradation of the GFP in the case of TcGFPAVP1. In order to study this situation, the vacuolar-deficient yeast mutant BJ5457 [24] was transformed with plasmids pAVP1, pTcAVP1 and pTcGFPAVP1 and total membrane preparations obtained with the resulting strains were analysed and compared with preparations obtained with YPC4 cells transformed with the same plasmids. Immunochemical analysis strongly suggested that vacuolar proteases are involved in the processing of AVP1 and chimaeric derivatives observed in mutant YPC4. These results along with the membrane-associated PPase activity data further support the idea that, although AVP1 and TcAVP1 can be found in YPC4 vacuoles, a high proportion of these polypeptides is subjected to proteolysis. This effect is much smaller in the case of TcGFPAVP1, thus suggesting that the combination of the *T. cruzi* H^+-PPase N-terminal signal peptide and yEGFP is more efficient than the signal peptide alone at altering the subcellular distribution of the resulting chimaera. Fluorescence microscopy supported the data obtained by immunodetection and activity assays, thus, unlike in mutant BJ5457, the green fluorescence corresponding to TcGFPAVP1 in mutant YPC4 showed a pattern not clearly associated to the vacuolar membrane. There are two contributions to this effect according to our results: on the one hand, a significant fraction of TcGFPAVP1 is targeted to other internal membranes and, on the other hand, the polypeptide located in the vacuolar membrane is subjected to proteolysis so that most of the GFP moiety is degraded. Therefore, the role of vacuolar proteases provides an explanation of why the fluorescence associated with GFP is not located in the vacuolar membrane and further suggests that the proton pump responsible for the acidification of the vacuole in YPC4 cells transformed with pTcGFPAVP1 is actually a native-like AVP1 protein and not the chimaeric derivative.

Altogether, our results show that the PPi-dependent proton pump AVP1 can alleviate the most characteristic phenotypes associated to the lack of V-ATPase in yeast, especially when the former is preferentially targeted to internal membranes by attaching an appropriate signal peptide to its N-terminus [21] . In the opinion of the authors, this is the first direct proof that a H^+-translocating PPase can sustain growth and significant acidification of intracellular lumina in the absence of any V-ATPase activity.

These results raise another question related to the occurrence of two proton pumps in the same subcellular location in certain organisms, one of them being an extremely complex molecular machinery (the V-ATPase) and the other a much simpler membrane pump. There are numerous recent data supporting that V-ATPases may play more roles than the acidification of internal compartments, such as the participation of the V_0 domain in membrane fusion [41] and others [42]. On the other hand, the V-ATPase complex may offer many more possibilities of activity modulation and, thus, may be more finely tuned than the comparatively simpler H^+-PPase. Additionally, reports of co-regulation and physical interactions between V-ATPases and H^+-PPases in plant tonoplast may complicate further the task of discriminate the respective roles of both pumps [18]. A yeast expression system like

the one in the present work can help ascertaining the importance of different V-ATPase polypeptides or whole domains in moonlighting functions independent of lumen acidification.

In any case, the H^+-PPases probably imply an adaptive advantage to the organisms where they occur because they offer an alternative pump to generate proton gradients in internal organelles by using an abundant by-product of anabolism, inorganic pyrophosphate. [43]. This is likely to be a critical issue under conditions that require the optimisation of cellular energy usage. In this respect, it is worthwhile pointing out that the H^+-PPase seems to be the main tonoplast pump in other plant systems, such as grape berry cells [44] .

The yeast system described in the present work may have biotechnological applications, thus, it is a good experimental system to accomplish studies of random mutagenesis aimed at obtaining enhanced versions of AVP1 and other PPi-dependent ion pumps. On the other hand, YPC4 transformed with diverse H^+-PPases might be a useful system to check for possible roles other than the acidification of internal organelles proposed for fungal and animal V-ATPases and it may be a suitable system to study the effect of H^+-PPases inhibitors *in vivo*, as these proton pumps occur in miccroorganisms responsible of diseases such as malaria, leishmaniasis, Chagas disease and sleeping sickness [15, 45]. Finally, this experimental system envisages novel ways of engineering cell tolerance to macrolides, a class of drugs of increasing relevance in therapeutics of a range of diseases in which cellular proton homeostasis may play crucial roles, such as cancer.

REFERENCES

1 Kane, P. M. (2006) The where, when, and how of organelle acidification by the yeast vacuolar H^+-ATPase. Microbiol. Mol. Biol. Rev. **70**, 177-191

2 Nishi, T. and Forgac, M. (2002) The vacuolar (H+)-ATPases--nature's most versatile proton pumps. Nat. Rev. Mol. Cell Biol. **3**, 94-103

3 Forgac, M. (2007) Vacuolar ATPases: rotary proton pumps in physiology and pathophysiology. Nat. Rev. Mol. Cell Biol. **8**, 917-929

4 Hernández, A., Serrano, G., Herrera-Palau, R., Pérez-Castiñeira, J. R. and Serrano, A. Intraorganellar acidification by V-ATPases: a target in cell proliferation and cancer therapy. Recent Pat. Anticancer Drug Discov. **5**, 88-98

5 Bowman, E. J., Siebers, A. and Altendorf, K. (1988) Bafilomycins: a class of inhibitors of membrane ATPases from microorganisms, animal cells, and plant cells. Proc. Natl. Acad. Sci. U S A. **85**, 7972-7976

6 Bowman, E. J., Graham, L. A., Stevens, T. H. and Bowman, B. J. (2004) The bafilomycin/concanamycin binding site in subunit c of the V-ATPases from *Neurospora crassa* and *Saccharomyces cerevisiae*. J. Biol. Chem. **279**, 33131-33138

7 Nelson, H. and Nelson, N. (1990) Disruption of genes encoding subunits of yeast vacuolar H(+)-ATPase causes conditional lethality. Proc. Natl. Acad. Sci. U S A. **87**, 3503-3507

8 Ohya, Y., Umemoto, N., Tanida, I., Ohta, A., Iida, H. and Anraku, Y. (1991) Calcium-sensitive *cls* mutants of *Saccharomyces cerevisiae* showing a Pet- phenotype are ascribable to defects of vacuolar membrane H(+)-ATPase activity. J. Biol. Chem. **266**, 13971-13977

9 Ramsay, L. M. and Gadd, G. M. (1997) Mutants of *Saccharomyces cerevisiae* defective in vacuolar function confirm a role for the vacuole in toxic metal ion detoxification. FEMS Microbiol. Lett. **152**, 293-298

10 Hinton, A., Bond, S. and Forgac, M. (2009) V-ATPase functions in normal and disease processes. Pflugers Arch. **457**, 589-598

11 Morel, N. (2003) Neurotransmitter release: the dark side of the vacuolar-H^+ATPase. Biol. Cell. **95**, 453-457
12 Drozdowicz, Y. M. and Rea, P. A. (2001) Vacuolar H(+) pyrophosphatases: from the evolutionary backwaters into the mainstream. Trends Plant Sci. **6**, 206-211
13 Maeshima, M. (2001) TONOPLAST TRANSPORTERS: Organization and Function. Annu. Rev. Plant Physiol. Plant Mol. Biol. **52**, 469-497
14 Serrano, A., Pérez-Castiñeira, J. R., Baltscheffsky, M. and Baltscheffsky, H. (2007) H^+-PPases: yesterday, today and tomorrow. IUBMB Life. **59**, 76-83
15 Docampo, R., de Souza, W., Miranda, K., Rohloff, P. and Moreno, S. N. (2005) Acidocalcisomes - conserved from bacteria to man. Nat. Rev. Microbiol. **3**, 251-261
16 Pérez-Castiñeira, J. R., López-Marqués, R. L., Losada, M. and Serrano, A. (2001) A thermostable K(+)-stimulated vacuolar-type pyrophosphatase from the hyperthermophilic bacterium *Thermotoga maritima*. FEBS Lett. **496**, 6-11
17 Pérez-Castiñeira, J. R., Gómez-García, R., López-Marqués, R. L., Losada, M. and Serrano, A. (2001) Enzymatic systems of inorganic pyrophosphate bioenergetics in photosynthetic and heterotrophic protists: remnants or metabolic cornerstones? Int. Microbiol. **4**, 135-142
18 Schumacher, K. (2006) Endomembrane proton pumps: connecting membrane and vesicle transport. Curr. Opin. Plant Biol. **9**, 595-600
19 Kim, E. J., Zhen, R. G. and Rea, P. A. (1994) Heterologous expression of plant vacuolar pyrophosphatase in yeast demonstrates sufficiency of the substrate-binding subunit for proton transport. Proc. Natl. Acad. Sci. U S A. **91**, 6128-6132
20 Hill, J. E., Scott, D. A., Luo, S. and Docampo, R. (2000) Cloning and functional expression of a gene encoding a vacuolar-type proton-translocating pyrophosphatase from *Trypanosoma cruzi*. Biochem. J. **351**, 281-288
21 Drake, R., Serrano, A. and Pérez-Castiñeira, J. R. (2010) N-terminal chimaeras with signal sequences enhance the functional expression and alter the subcellular localization of heterologous membrane-bound inorganic pyrophosphatases in yeast. Biochem. J. **426**, 147-157
22 Ros, R., Montesinos, C., Rimon, A., Padan, E. and Serrano, R. (1998) Altered Na^+ and Li^+ homeostasis in *Saccharomyces cerevisiae* cells expressing the bacterial cation antiporter NhaA. J. Bacteriol. **180**, 3131-3136
23 Kane, P. M., Yamashiro, C. T., Wolczyk, D. F., Neff, N., Goebl, M. and Stevens, T. H. (1990) Protein splicing converts the yeast *TFP1* gene product to the 69-kD subunit of the vacuolar H(+)-adenosine triphosphatase. Science. **250**, 651-657
24 Jones, E. W. (1991) Tackling the protease problem in *Saccharomyces cerevisiae*. Methods Enzymol. **194**, 428-453
25 Schiestl, R. H. and Gietz, R. D. (1989) High efficiency transformation of intact yeast cells using single stranded nucleic acids as a carrier. Curr. Genet. **16**, 339-346
26 Yenush, L., Mulet, J. M., Arino, J. and Serrano, R. (2002) The Ppz protein phosphatases are key regulators of K^+ and pH homeostasis: implications for salt tolerance, cell wall integrity and cell cycle progression. EMBO J. **21**, 920-929
27 Treco, D. A. and Lunblad, V. (1993) Preparation of yeast media. Curr. Protoc. Mol. Biol. Unit **13.1**
28 Pérez-Castiñeira, J. R., López-Marqués, R. L., Villalba, J. M., Losada, M. and Serrano, A. (2002) Functional complementation of yeast cytosolic pyrophosphatase by bacterial and plant H^+-translocating pyrophosphatases. Proc. Natl. Acad. Sci. U S A. **99**, 15914-15919
29 Conibear, E. and Stevens, T. H. (2002) Studying yeast vacuoles. Methods Enzymol.

351, 408-432
30 Roberts, C. J., Raymond, C. K., Yamashiro, C. T. and Stevens, T. H. (1991) Methods for studying the yeast vacuole. Methods Enzymol. **194**, 644-661
31 Lenoir, G., Menguy, T., Corre, F., Montigny, C., Pedersen, P. A., Thines, D., le Maire, M. and Falson, P. (2002) Overproduction in yeast and rapid and efficient purification of the rabbit SERCA1a Ca(2+)-ATPase. Biochim. Biophys. Acta. **1560**, 67-83
32 Rathbun, W. B. and Betlach, M. V. (1969) Estimation of enzymically produced orthophosphate in the presence of cysteine and adenosine triphosphate. Anal. Biochem. **28**, 436-445
33 Pérez-Castiñeira, J. R. and Apps, D. K. (1990) Vacuolar H(+)-ATPase of adrenal secretory granules. Rapid partial purification and reconstitution into proteoliposomes. Biochem. J. **271**, 127-131
34 Valverde, F., Losada, M. and Serrano, A. (1997) Functional complementation of an *Escherichia coli* gap mutant supports an amphibolic role for NAD(P)-dependent glyceraldehyde-3-phosphate dehydrogenase of *Synechocystis* sp. strain PCC 6803. J. Bacteriol. **179**, 4513-4522
35 López-Marqués, R. L., Pérez-Castiñeira, J. R., Buch-Pedersen, M. J., Marco, S., Rigaud, J. L., Palmgren, M. G. and Serrano, A. (2005) Large-scale purification of the proton pumping pyrophosphatase from *Thermotoga maritima*: a "Hot-Solve" method for isolation of recombinant thermophilic membrane proteins. Biochim. Biophys. Acta. **1716**, 69-76
36 Bradford, M. M. (1976) A rapid and sensitive method for the quantitation of microgram quantities of protein utilizing the principle of protein-dye binding. Anal. Biochem. **72**, 248-254
37 Perzov, N., Padler-Karavani, V., Nelson, H. and Nelson, N. (2002) Characterization of yeast V-ATPase mutants lacking Vph1p or Stv1p and the effect on endocytosis. J. Exp. Biol. **205**, 1209-1219
38 Jasti, J., Furukawa, H., Gonzales, E. B. and Gouaux, E. (2007) Structure of acid-sensing ion channel 1 at 1.9 A resolution and low pH. Nature. **449**, 316-323
39 Sato, K., Sato, M. and Nakano, A. (2001) Rer1p, a retrieval receptor for endoplasmic reticulum membrane proteins, is dynamically localized to the Golgi apparatus by coatomer. J. Cell Biol. **152**, 935-944
40 Mertens, E. (1991) Pyrophosphate-dependent phosphofructokinase, an anaerobic glycolytic enzyme? FEBS Lett. **285**, 1-5
41 Baars, T. L., Petri, S., Peters, C. and Mayer, A. (2007) Role of the V-ATPase in regulation of the vacuolar fission-fusion equilibrium. Mol. Biol. Cell. **18**, 3873-3882
42 Gaxiola, R. A., Palmgren, M. G. and Schumacher, K. (2007) Plant proton pumps. FEBS Lett. **581**, 2204-2214
43 López-Marqués, R. L., Pérez-Castiñeira, J. R., Losada, M. and Serrano, A. (2004) Differential regulation of soluble and membrane-bound inorganic pyrophosphatases in the photosynthetic bacterium *Rhodospirillum rubrum* provides insights into pyrophosphate-based stress bioenergetics. J. Bacteriol. **186**, 5418-5426
44 Fontes, N., Silva, R., Vignault, C., Lecourieux, F., Geros, H. and Delrot, S. Purification and functional characterization of protoplasts and intact vacuoles from grape cells. BMC Res. Notes. **3**, 19
45 Pérez-Castiñeira, J. R., Alvar, J., Ruíz-Pérez, L. M. and Serrano, A. (2002) Evidence for a wide occurrence of proton-translocating pyrophosphatase genes in parasitic and free-living protozoa. Biochem. Biophys. Res. Commun. **294**, 567-573
46 Thomas, B. J. and Rothstein, R. (1989) Elevated recombination rates in

transcriptionally active DNA. Cell. **56**, 619-630

AUTHOR CONTRIBUTION

J. R. Pérez-Castiñeira carried out most of the experimental work and wrote the manuscript, A. Hernández generated YPC4 mutant and corrected the manuscript, R. Drake performed preliminary studies and A. Serrano supervised the work and the final version of the manuscript.

ACKNOWLEDGEMENTS

The authors deeply thank Prof. Ramón Serrano (Univ. Politécnica de Valencia, Spain) for providing anti-Pma1p antibody and yeast mutant strain RS-1144 and Prof. Andrés Aguilera (Universidad de Sevilla, Spain) for providing yeast strain BJ5457. We also thank Dr. Alicia Orea for excellent technical assistance with fluorescence microscopy and Ms. Isabel Jiménez for yeast culturing.

FUNDING

Authors thank the Regional Andalusian Goverment and the Spanish Ministerio de Ciencia e Innovación for their financial support to PAIDI group BIO-261 and for research grants P07-CVI-03082, BFU2007-61887 and BFU2010-15622, all of them partially funded by the EU FEDER (Fondo Europeo de Desarrollo Regional) program.

LEGENDS OF FIGURES

Fig. 1. Drop tests of yeast mutant YPC3 cells grown in the presence of the macrolide inhibitor bafilomycin A1 at pH 5.5 and 8.0 (A) and in the presence of 100 mM $CaCl_2$ or 4 mM $ZnCl_2$ at pH 5.5 (B).
Cells were transformed with plasmids pRS699b (Control-), pIPP1, pAVP1, pTcAVP1 and pTcGFPAVP1 and grown as described in Materials and Methods. Serial dilutions of the cultures were made in sterile water and spotted onto YPGal and YPD plates containing 2 µM bafilomycin A1 and buffered at the indicated pH values with 50 mM MES-TRIS. Plates containing Ca^{2+} and Zn^{2+} salts were adjusted to pH 5.5 with the same buffer. In panel **A** 1:10, 1:100 and 1:1000 serial dilutions are shown. In panel **B** 1:10 and 1:100 dilutions are shown. Growth was recorded after two days at 30 ºC in all cases except for Zn^{2+} plates, that were grown for four days. No sensitivity to pH 8 or to Ca^{2+} or Zn^{2+} was observed for YPC3 cells in the absence of bafilomycin A1 (not shown).

Fig. 2. Drop tests of yeast mutant YPC4 cells grown at pH 5.5, 7.5 and 8.0 (A) and in the presence of 100 mM $CaCl_2$ or 4 mM $ZnCl_2$ at pH 5.5 (B).
Cells were transformed with plasmids pRS699b (Control-), pIPP1, pAVP1, pTcAVP1, pTcGFPAVP1 and pVMA1 and grown as described in Materials and Methods. Serial dilutions of the cultures were made in sterile water and spotted onto YPGal and YPD plates buffered at the indicated pH values with 50 mM MES-TRIS. Plates containing Ca^{2+} and Zn^{2+} salts were adjusted to pH 5.5 with the same buffer. In panel **A** 1:10, 1:100 and 1:1000 serial dilutions are shown. In panel **B** 1:10 and 1:100 dilutions are shown. Growth was recorded after four days

in all cases except for those at pH 8, grown for seven days.

Fig. 3. Vacuolar acidification of transformed YPC4 cells studied by accumulation of quinacrine.
Cells were transformed with the indicated plasmids and grown as described in Materials and Methods. Vacuole acidification was assessed by accumulation of the fluorescent probe quinacrine as described elsewhere [28]. Cells were visualised in a Leica DM6000B microscope. Left column shows differential interference contrast microscopy (DIC) of a typical field of transformed YPC4 cells, central column shows the pattern of quinacrine accumulation (observed with a FITC green filter) in the same cells and right column shows the overlap of both.

Fig. 4. Endocytic internalization of the fluorescent marker FM4-64 in transformed YPC4 cells.
The rate of endocytosis was studied by incubating transformed YPC4 cells grown to early log phase with FM4-64 during 15 min, as previously described [28]. Cells were then transferred to YPD and visualised as in Fig. 3 after 30 minutes of incubation with the fluorescent dye. In panel **A**, left column shows DIC microscopy of a typical field of transformed YPC4 cells, central column shows the pattern of FM4-64 labelling in the same cells and right column shows the overlap of both. Panel **B** shows YPC4 cells transformed with plasmid pTcGFPAVP1. From left to right: visualisation of the cells by DIC microscopy, with Red (Texas Red) and green (FITC) filters, overlap of red and green filter microphotographs, and overall overlap of the tree former microphotographs.

Fig. 5. PPi- and ATP-dependent proton pumping activity measured as quenching of ACMA fluorescence (A), membrane associated PPi hydrolysis activity (B) and Western blot analyses (C) of vacuolar membrane preparations obtained from transformed YPC4 cells.
(A) Proton translocation activity was measured by recording the PPi-dependent (left) and ATP-dependent (right) ACMA fluorescence quenching. Upper panel shows typical traces obtained in these experiments; below, initial rates of fluorescence quenching *vs.* time for the different preparations are plotted. Values are means $\pm$ S.E. of three independent experiments (n=3) and asterisks indicate differences that are statistically significant ($P < 0.005$). n.d.: not detected activity. Approximately 30 µg of protein were utilized for these assays. **(B)** Specific PPi hydrolysis activity associated with vacuolar membranes obtained from YPC4 cells transformed with the different plasmids tested. Activity values shown are means $\pm$ S.E. (n=3) using preparations obtained from YPC4 cells transformed with pRS699b as a reference. Asterisks indicate differences that are statistically significant ($P < 0.005$). White and black bars represent activities in the absence and presence of potassium chloride, respectively. n.d.: not detected activity. **(C)** Immunodetection of AVP1 (upper panel) and yeast Vma1p in vacuolar membranes of transformed YPC4 cells. Approx. 30 µg of protein were loaded per lane. Asterisks indicate bands associated with chimaeric protein TcGFPAVP1 (approx. 120 kDa) and AVP1 (72 kDa).

Fig. 6. Western blot analysis (A) and membrane-associated PPi hydrolysis activity (B) of total membrane preparations obtained from transformed YPC4 and BJ5457 cells and fluorescence microscopy visualization of YPC4 and BJ5457 cells transformed with pTcGFPAVP1 (C).

(A) Immunodetection of AVP1 and derivatives with antibodies against a membrane-bound PPase (anti-TVP, upper panel) and GFP (anti-GFP) in total membranes of YPC4 (left) and BJ5457 (right) cells transformed with plasmids pRS699b, pIPP1, pAVP1, pTcAVP1 and pTcGFPAVP1. Approx. 70 µg of protein were loaded per lane. Asterisks indicate bands associated with chimaeric protein TcGFPAVP1 (approx. 120 kDa) and AVP1 (72 kDa). **(B)** Specific PPi hydrolysis activity associated with total membranes obtained from YPC4 and BJ5457 cells transformed with the different plasmids tested. Activity values shown are means ± S.E. (n=3) using preparations obtained from cells transformed with pRS699b as reference. Asterisks indicate differences that are statistically significant ($P < 0.005$). White and black bars represent activities in the absence and presence of potassium chloride, respectively. n.d.: not detected activity. **(C)** YPC4 and BJ5457 cells were transformed with plasmid pTcGFPAVP1 and visualised in a Leica DM6000B microscope. Left column shows differential interference contrast microscopy (DIC) of a typical field of cells, central column shows the pattern of green fluorescence distribution (FITC green filter) in the same cells and right column shows the overlap of both. White arrowheads indicate vacuolar membranes.

Biochemical Journal Immediate Publication. Published on 26 May 2011 as manuscript BJ20110447

Figure 1

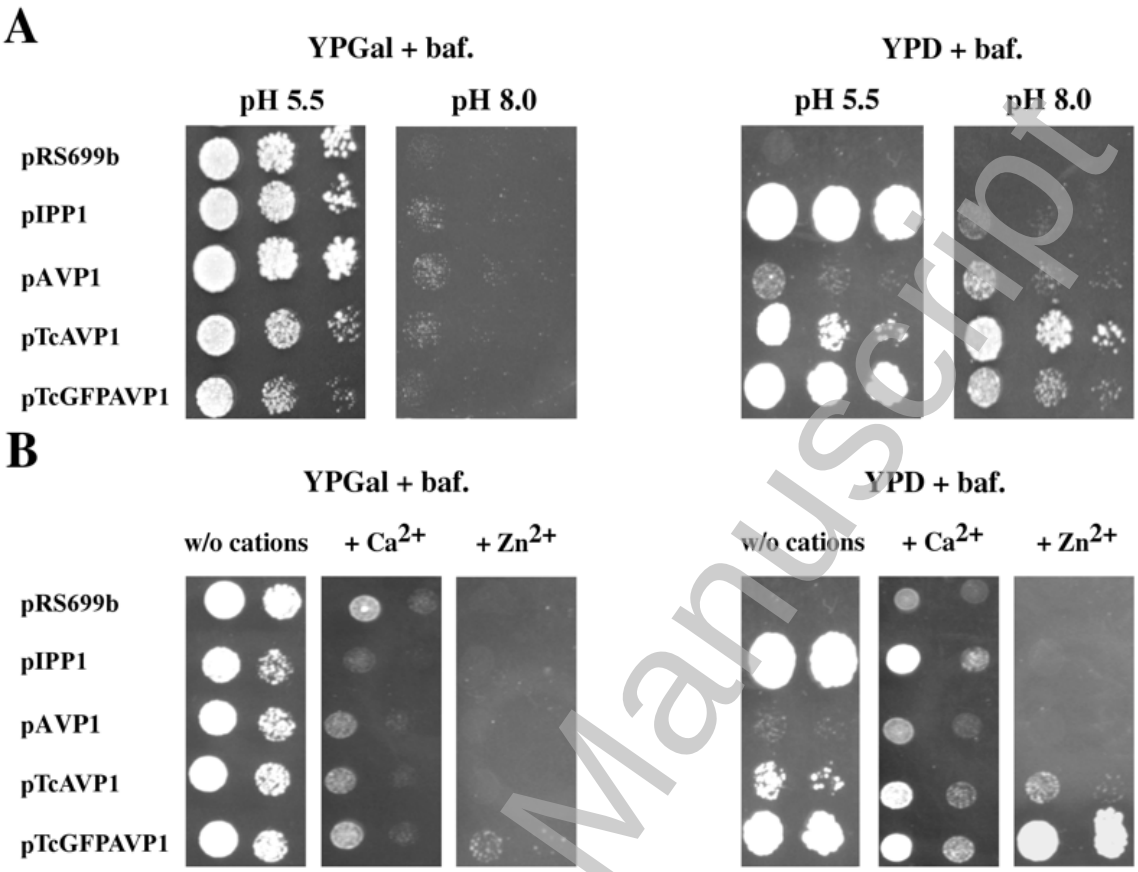

Figure 2

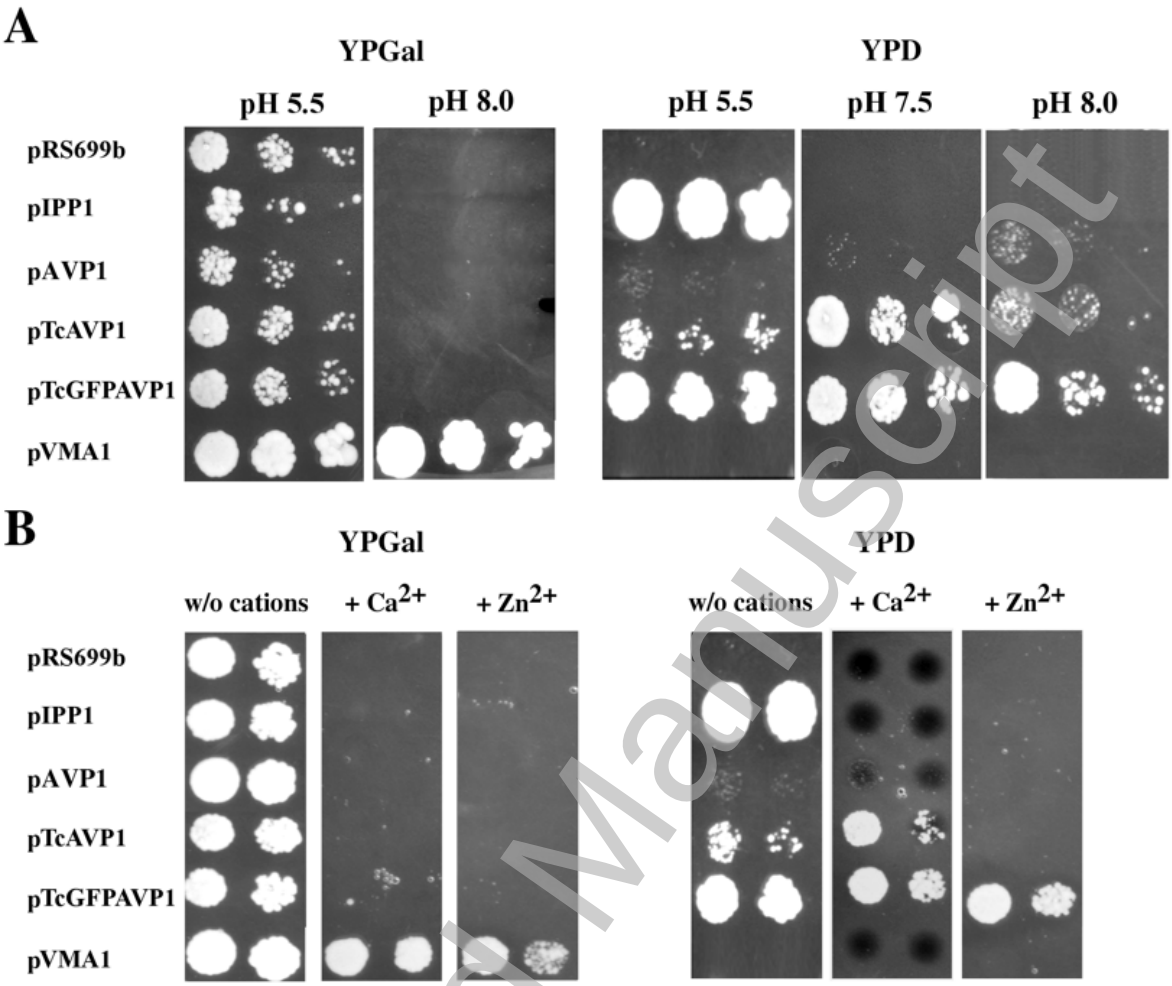

Biochemical Journal Immediate Publication. Published on 26 May 2011 as manuscript BJ20110447

Figure 3

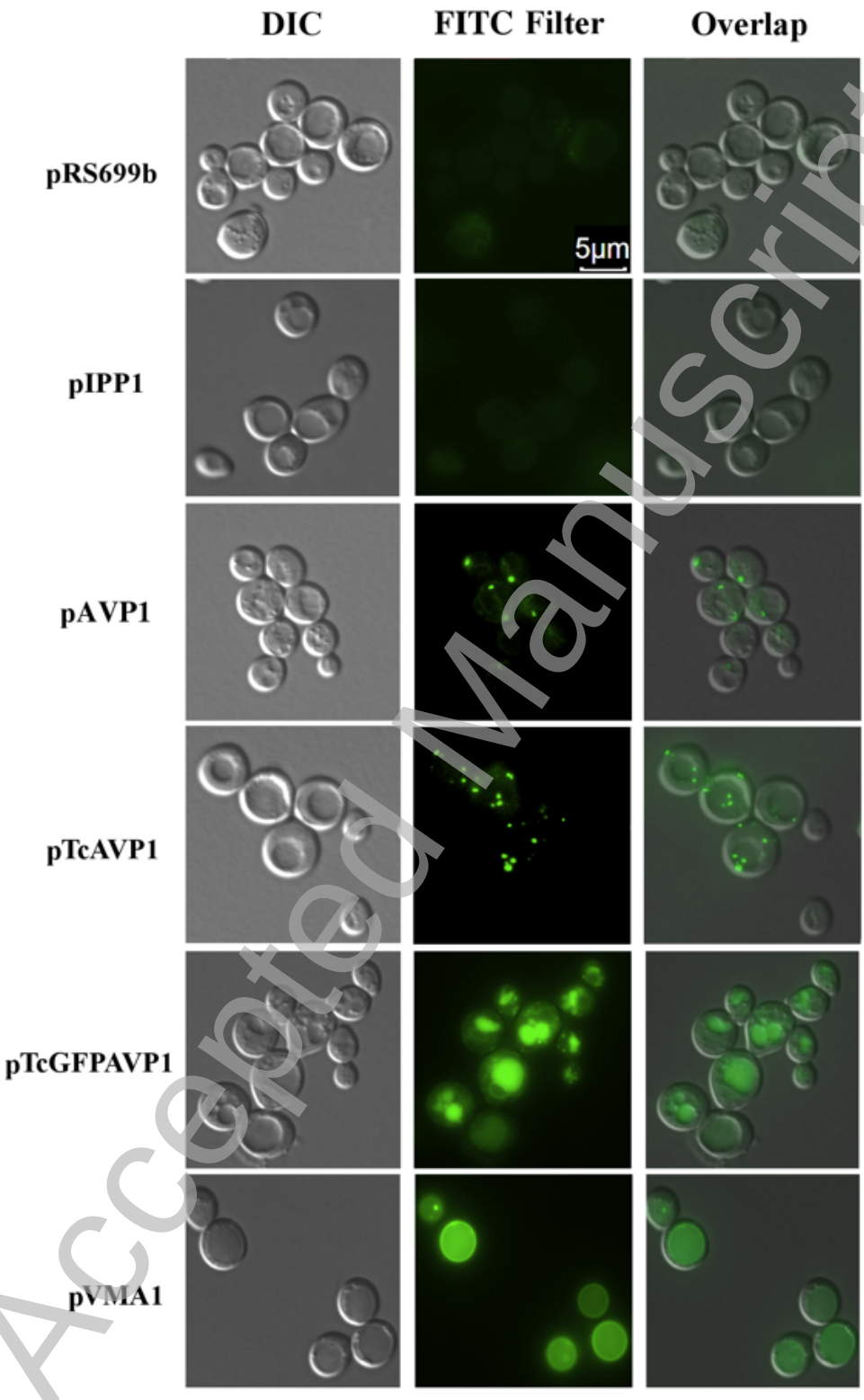

Biochemical Journal Immediate Publication. Published on 26 May 2011 as manuscript BJ20110447

Figure 4

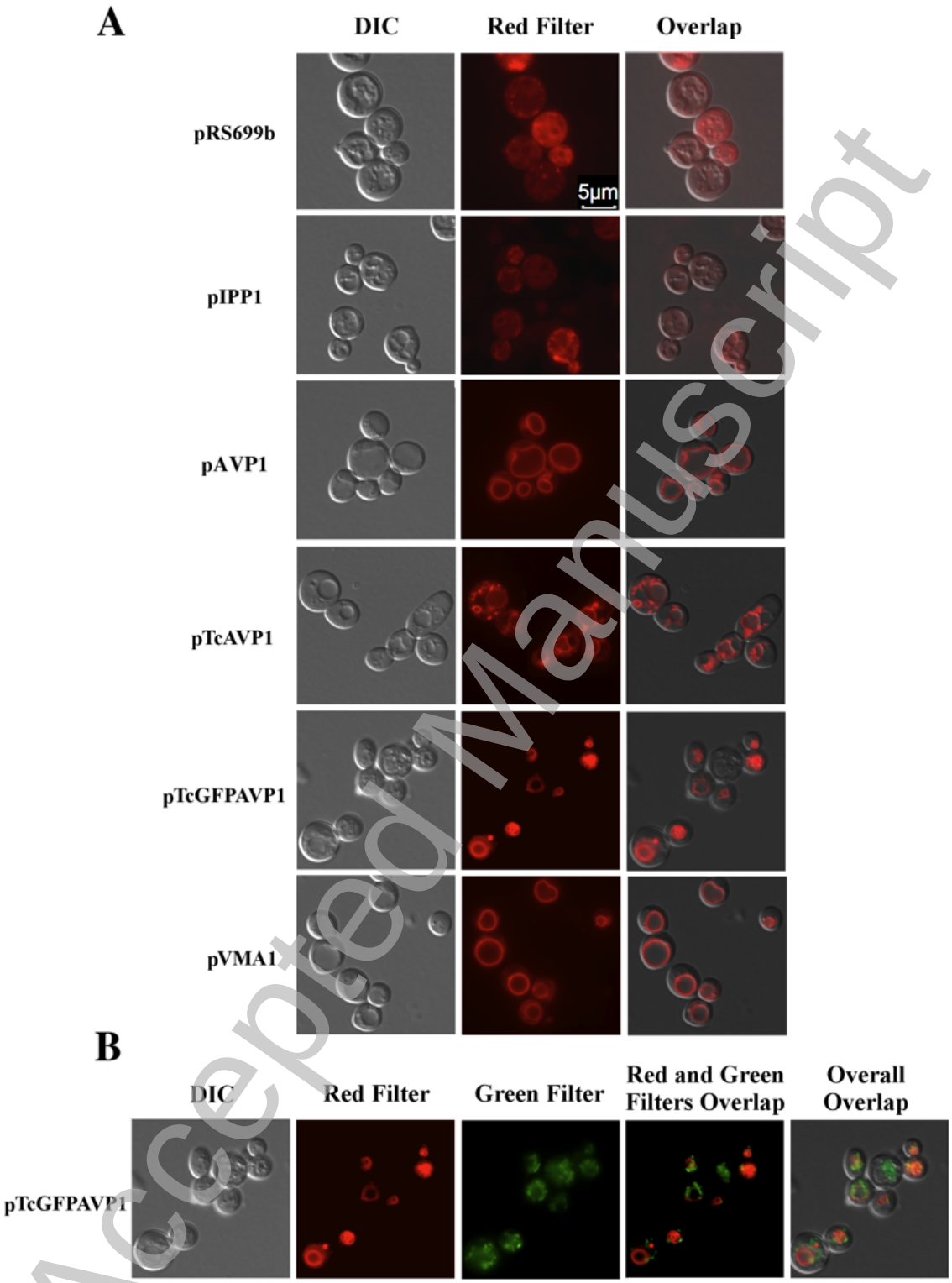

Figure 5

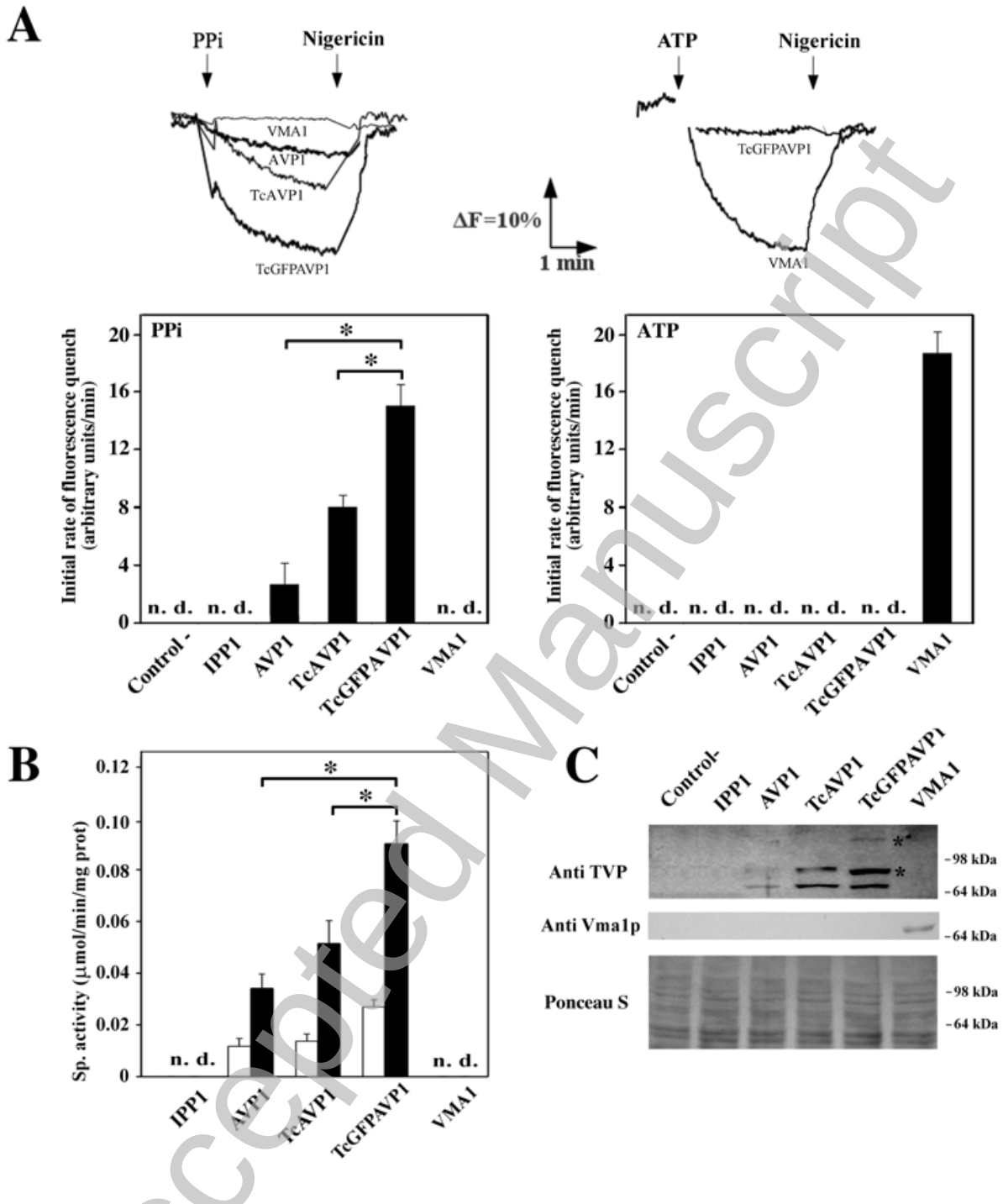

Figure 6